DOI: 10.1002/ejic.201001132

Synthesis and Characterization of Nickel(II) Aminoalkoxides: Application to Molecular Precursors for MOCVD of Ni Thin Films

Seung Ho Yoo,[a] Hana Choi,[a] Hyo-Suk Kim,[a] Bo Keun Park,[a] Sun Sook Lee,[a] Ki-Seok An,[a] Young Kuk Lee,[a] Taek-Mo Chung,[a] and Chang Gyoun Kim*[a]

Keywords: Nickel / N,O ligands / Chemical vapor deposition / Thin films

Novel single precursors for Ni, Ni(dmamp)$_2$ (**1**), Ni(deamp)$_2$ (**2**), and Ni(emamp)$_2$ (**3**), were synthesized by the metathesis reaction between [Ni(NH$_3$)$_6$]Cl$_2$ and two equiv. of Na(dmamp), Na(deamp), and Na(emamp), respectively. Complexes **1**–**3** have been characterized by IR, ^{1}H NMR, and ^{13}C NMR spectroscopies, and microanalytical data, as well as single-crystal X-ray diffraction studies. Through GC/MS analysis of the gaseous species generated by the decomposition of **1**, a self-reduction pathway to form metallic Ni was studied. By the metalorganic chemical vapor deposition of **1**, metallic Ni hexagonal-phase thin films were obtained at 250 °C and cubic-phase thin films were obtained at 400 °C.

Introduction

Nickel has been used for various thin-film materials, often alloyed with other elements. Nickel thin films have been applied as materials for protective coatings against oxidation and corrosion as decorative and selective absorbers.[1] Nickel silicides are in the limelight as a contact material in semiconductor devices.[2,3] Nickel oxides can be applied to *p*-type transparent conducting films, chemical sensors, electrochromic devices, and resistive random access memory (ReRAM) devices due to their optical, electrical, and magnetic properties.[4–8] Nickel sulfides and nickel selenides as *p*-type semiconductors and nickel phosphides as an n-type semiconductor are useful for electrodes in photoelectrochemical storage devices.[9,10] Various nickel-based alloys as thin films can be used in catalysts, optical materials, magnetic materials, hydrogen storage, resistive and thermoelectric devices, and micro/nano-electromechanical systems.[11–22]

Nickel films have been deposited by metalorganic chemical vapor deposition (MOCVD) or atomic layer deposition (ALD) processes with precursors such as Ni(CO)$_4$,[23–25] nickelocenes,[26–29] nickel(II) β-diketonate complexes,[30–33] and Ni[MeC(N*i*Pr)$_2$]$_2$.[34,35] These precursors suffer from toxicity, low vapor pressure, poor thermal stability, and incorporation of impurities such as oxygen or carbon from the ligand or H_2 necessary as a reducing agents for Ni metal preparation. Recently, NiN_x films were prepared using Ni[MeC(N*i*Bu)$_2$]$_2$ as the precursor; Ni films were then formed by reduction of the NiN_x films by annealing in H_2 at 160 °C or with H_2 plasma at room temperature.[36] Therefore, it is necessary that a novel precursor, which is more readily decomposed and volatile than the well-known nickel precursors and lessens the incorporation of impurities, should be designed and synthesized.

MOCVD and ALD methods have been used for various thin-film materials in the microelectronic area.[37,38] To apply these methods for thin-film manufacture, adequate precursors should be prepared, thus it is necessary for the development of precursors and the understanding of their characteristics. Precursors for MOCVD and ALD must be volatile, transportable, thermally stable at evaporation temperatures, readily decompose at relatively low substrate temperatures, non-toxic, non-corrosive, cheap, and highly pure.[39–41] Our research has been focused on the development of novel precursors for MOCVD and ALD and preparation of metal and metal oxide thin films using these precursors by MOCVD and ALD techniques.[42–48]

In this work, we synthesized novel Ni^{II} aminoalkoxide complexes using various dialkylamino alcohols ligands, namely, 1-(dimethylamino)-2-methyl-2-propanol (dmampH), 1-(diethylamino)-2-methyl-2-propanol (deampH), and 1-(ethylmethylamino)-2-methyl-2-propanol (emampH), and characterized each by spectroscopic methods and X-ray single crystallography. From our preliminary CVD studies, the nickel aminoalkoxide complexes were appropriate as precursors for the deposition of nickel films without external reducing agents such as hydrogen. To elucidate the CVD reaction pathway, ex-situ GC/MS experiments of the decomposed by-products were performed.

[a] Advanced Materials Division, Korea Research Institute of Chemical Technology,
Yuseong, P.O. Box 107, Daejeon 305-600, South Korea
Fax: +82-42-861-4151
E-mail: cgkim@krict.re.kr

Supporting information for this article is available on the WWW under http://dx.doi.org/10.1002/ejic.201001132.

Results and Discussion

Synthesis and Characterization of 1–3

As shown in Scheme 1, the nickel(II) aminoalkoxides were synthesized by the metathesis reaction between $[Ni(NH_3)_6]Cl_2$ and two equiv. of the sodium aminoalkoxides; all complexes were purified by sublimation (**1**: 70 °C, **2**: 70 °C, and **3**: 45 °C at 10^{-2} Torr). This reaction is similar to the synthesis of $Ni(dmap)_2$ (dmap = 1,2-dimethylamino-2-propoxide), which is purified by sublimation at 93–95 °C at 10^{-2} Torr.[49] The complexes were highly soluble in organic solvents such as THF, Et_2O, and toluene and were characterized by a combination of FT-IR, ^1H NMR, and ^{13}C NMR spectroscopies, elemental analysis, MS spectrometry, and X-ray single crystallography. Mass spectrometric data of all complexes displayed only monomeric fragments such as $[Ni(L)_2]^+$ and $[Ni(L)_1]^+$ species. On the basis of mass data, we inferred that the complexes were monomers with four-coordinate metal spheres, which was confirmed by X-ray single crystallographic analysis.

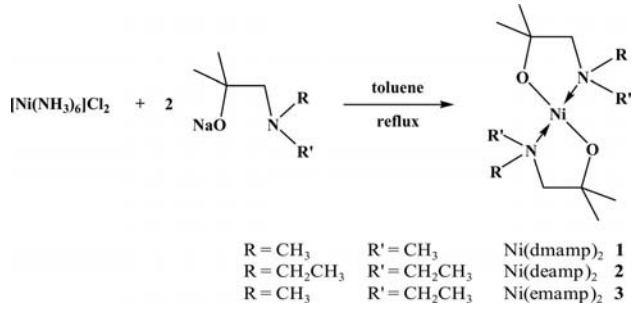

Scheme 1. Synthesis of complexes **1**–**3**.

The melting points of the complexes were measured by a melting point apparatus (model No. SMP3 manufactured by Bibby Sterilin) and appear at 118–120 °C for **1**, 52–53 °C for **2**, and 75–76 °C for **3**. The melting points of the complexes are lower than $NiCp_2$ (173 °C),[50] $Ni(acac)_2$ (240 °C),[51] $Ni(tmhd)_2$ (228 °C),[52] and $Ni(hfac)_2$ (207 °C).[53] The melting point of $Ni[MeC(NiPr)_2]_2$ (69 °C)[34] is higher than that of **2** and lower than those of **1** and **3**. On the other hand, the melting point of **1** is higher than that of $Ni[MeC(NiBu)_2]_2$ (87 °C).[36] The melting points of **1**–**3** were generally at lower temperature than known complexes except for those of few Ni precursors. The ^1H NMR spectrum of **1** showed three singlets at δ = 1.38 [-OC(CH_3)$_2$-], 1.73 [-CH_2N(CH_3)$_2$], and 2.32 ppm [-CH_2N(CH_3)$_2$]. These peaks are shifted by 0.2–0.3 ppm compared with those of dmampH (δ = 1.12, 2.04, and 2.12, respectively). The ^{13}C NMR spectrum of **1** has peaks present at δ = 32.6 [-OC(CH_3)$_2$-], 51.5 [-CH_2N(CH_3)$_2$], 73.6 [-OC(CH_3)$_2$-], and 78.3 ppm [-CH_2N(CH_3)$_2$] compared with dmampH (28.3, 48.2, 69.8, and 70.2, respectively).[54] The ^1H NMR spectrum of **2** showed two broad methylene peaks {2.43 [-N(CH_2CH_3)$_2$] and 3.01 [-N(CH_2CH_3)$_2$]}, whereas that of **3** has split broad peaks. These are thought to be due to relatively slow five-membered ring inversion.

X-ray Crystal Structures of 1–3

The single-crystal X-ray structure of **1** is shown in Figure 1. The nitrogen and oxygen atoms of the two dmamp ligands are chelated to the nickel atom of the square-planar structure in a *trans* geometry. The nickel atom forms an inversion center. The bond lengths of Ni1–O1 and Ni1–N1 are 1.837(3) and 1.937(3) Å, respectively, and are very similar to those of tetra-coordinated nickel complexes[54] and slightly longer than those of bis(β-ketoamino)nickel complexes.[55] They are shorter than the metal–atom distances reported in six-coordinate nickel(II) complexes.[56,57] The bite angle (87.74(13) Å) of the aminoalkoxide ligand is very similar to that found for $Ni(OCHMeCH_2NMe_2)_2$.[49] The bond angles O1–Ni1–N1 and O1′–Ni1–N1 are 87.74(13)° and 92.26(13)°, respectively, which are closed to the ideal 90° of a square plane. The two dmamp ligands and the nickel atom form a two five-membered ring metalacycle; the rings are composed of Ni1–O1–C1–C2–N1 and Ni1–O1′–C1′–C2′-N1′. These two five-membered rings have envelope conformations in which the C1 and C1′ atoms, each coordinating two methyl groups, are located out of the Ni1–O1–C2–N1 and Ni1–O1′–C2′–N1′ planes, respectively.

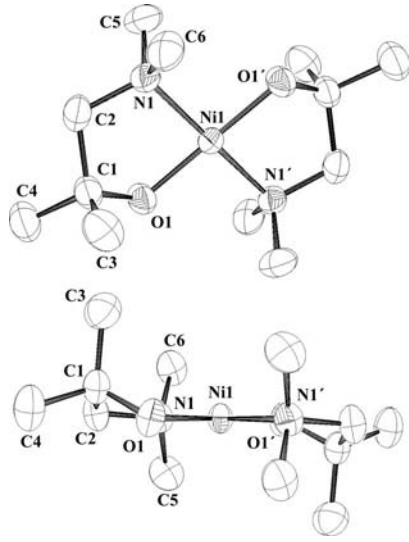

Figure 1. Molecular structure of **1**. Selected bond lengths [Å] and angles [°]: Ni(1)–O(1) 1.837(3), Ni(1)–N(1) 1.937(3), O(1)–C(1) 1.390(5), N(1)–C(2) 1.491(5), C(1)–C(2) 1.552(6); O(1)–Ni(1)–N(1) 87.74(13), O(1′)–Ni(1)–N(1) 92.26(13).

The molecular structures of **2** (Figure 2) and **3** (Figure 3) are similar to that of **1**. The structure of **2** includes two independent molecules (A and B) in an asymmetric unit; the Ni–O distances range from 1.8312(19) to 1.8433(18) Å and the Ni–N distances range from 1.951(2) to 1.955(2) Å. The Ni–O–N angles are in the range 88.11(9)–92.40(8)°. The bite angles are 88.57(9) and 88.39(8)° (molecule A), and 88.11(9) and 88.16(9)° (molecule B). In **3**, the Ni–O and Ni–N distances are 1.8434(9) and 1.9493(11) Å, respectively. The Ni–O–N angles are 88.26(5)° (O1–Ni1–N1) and 91.74(5)° (O1′–Ni1–N1), and the bite angle is 88.26(5)°. These two complexes also have two envelope conformational five-membered rings. In **2**, C1a and C3a (molecule

A), and C1b and C3b (molecule B) are located outside square planar plane. The C1 atom of **3** is also located at the same position.

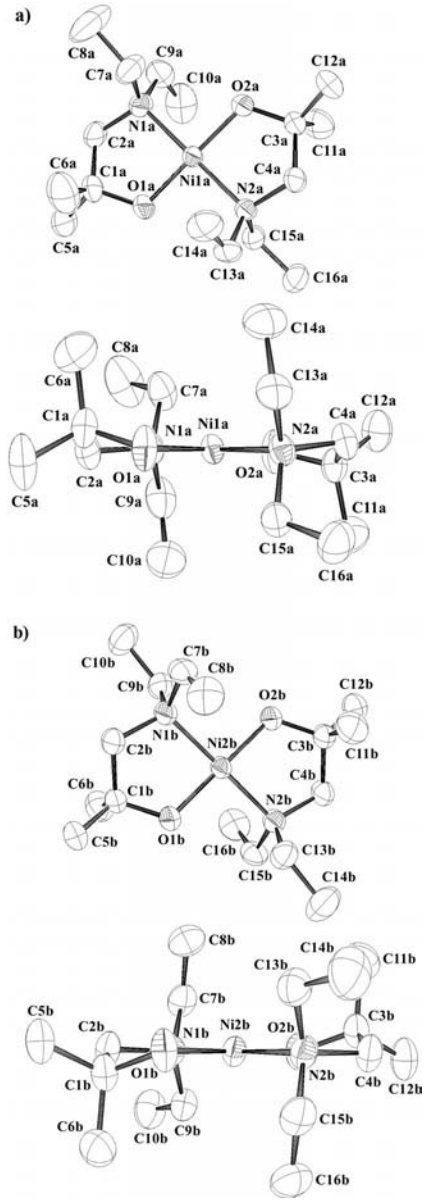

Figure 2. Molecular structure of **2**: a) molecule A and b) molecule B. Selected bond lengths [Å] and angles (°): molecule A: Ni(1A)–O(2A) 1.8312(19), Ni(1A)–O(1A) 1.8317(18), Ni(1A)–N(1A) 1.951(2), Ni(1A)–N(2A) 1.952(2), O(1A)–C(1A) 1.403(3), N(1A)–C(2A) 1.495(3), C(1A)–C(2A) 1.530(4); O(2A)–Ni(1A)–O(1A) 178.84(10), O(2A)–Ni(1A)–N(1A) 91.60(9), O(1A)–Ni(1A)–N(1A) 88.57(9), O(2A)–Ni(1A)–N(2A) 88.39(8), O(1A)–Ni(1A)–N(2A) 91.46(8), N(1A)–Ni(1A)–N(2A) 179.31(9); molecule B: Ni(2B)–O(1B) 1.8388(18), Ni(2B)–O(2B) 1.8433(18), Ni(2B)–N(1B) 1.955(2), Ni(2B)–N(2B) 1.954(2), O(1B)–C(1B) 1.405(3), N(1B)–C(2B) 1.505(3), C(1B)–C(2B) 1.543(4); O(2B)–Ni(2B)–O(1B) 179.36(9), O(2B)–Ni(2B)–N(1B) 92.40(8), O(1B)–Ni(2B)–N(1B) 88.11(9), O(2B)–Ni(2B)–N(2B) 88.16(8), O(1B)–Ni(2B)–N(2B) 91.33(9), N(1B)–Ni(2B)–N(2B) 179.24(9).

Complexes **1** and **3** have a dihedral angle of 0° between the Ni1–O1–N1 plane and the Ni1–O1′–N1′ plane due to an inversion center at the nickel atom. In complex **2** the dihedral angle is 0.4°.

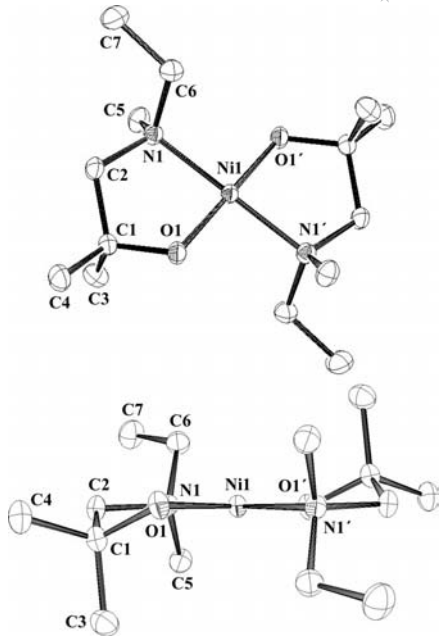

Figure 3. Molecular structure of **3**. Selected bond lengths (Å) and angles (°): Ni(1)–O(1) 1.8434(9), Ni(1)–N(1) 1.9493(11), O(1)–C(1) 1.4053(13), N(1)–C(2) 1.4973(14), C(1)–C(2) 1.5391(18); O(1)–Ni(1)–N(1) 88.26(5), O(1′)–Ni(1)–N(1) 91.74(5).

Thermal Analysis and Growth of Ni Films

The thermogravimetric analysis (TGA) of **1** is shown in Figure 4. Weight loss begins at 100 °C and is completed by 170 °C. Differential thermal analysis (DTA) shows an endothermic peak at 127 °C, attributed to the melting of **1**. An endothermic peak at 174 °C, accompanied by a weight loss (93%) is regarded as evaporation temperature of the complex.

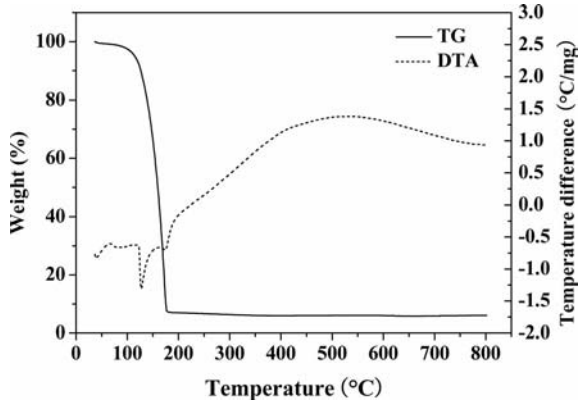

Figure 4. Thermal analysis of complex **1**.

The TGA of **2** and **3** exhibit weight losses that begin at about 100 °C and are complete by 200 °C (Figure 5). The amounts of the residues were 6% for **1**, and 20% each for **2** and **3**. The residual materials of the complexes were

thought to be oxidized materials, which were caused by exposure to air during the thermal experiments. The thermal property of **1** is better than those of **2** and **3**. TGA data of $Ni(acac)_2$, $Ni(acac)_2(en)$, and $Ni(tmhd)_2$ show weight losses at 120–250, 170–280, and 140–200 °C, respectively, and residues of 20.9, <1, and 4%.[58,59] Weight loss in $Ni[MeC(NiPr)_2]_2$ and $Ni[MeC(NiBu)_2]_2$ begin at about 100 °C and are complete by about 200 °C.[36] The amounts of residues were about 15 and < 1%, respectively. Volatility and thermal stability of **1** is better or similar compared with nickel(II) β-diketonates and nickel(II) amidinates complexes, therefore **1** is suitable as a MOCVD precursors to prepare metallic nickel thin films.

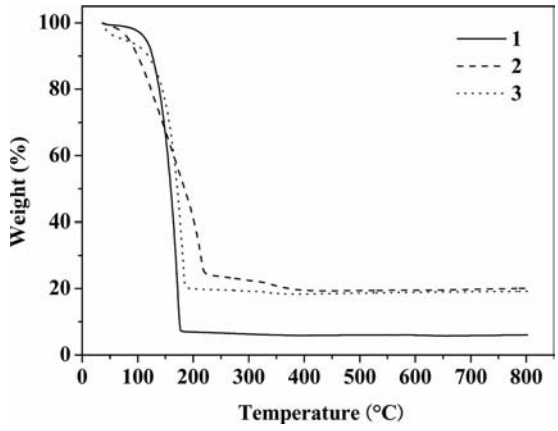

Figure 5. Comparison of thermogravimetric analysis of complexes **1**–**3**.

As a result of our preliminary CVD experiments, metallic nickel thin films were deposited from our precursors without using any reducing agent. Therefore, we thought that the growth of Ni films from **1** occurred through the self-reduction of the precursor. Unlike nickelocene or nickel(II) β-diketonate complexes, which require H_2 as a reducing agent for Ni metal preparation,[26–33] the Ni^{II} aminoalkoxides can be applied to deposit metallic Ni films without any reducing agents by a self-reduction reaction of the precursors at moderately low temperature. To elucidate the decomposition reaction pathway, we examined the gas phase by-products from the decomposition of **1**. The complex was decomposed in a tube furnace, which was filled with fragments of Si, and the decomposed gaseous products were collected in a liquid-nitrogen trap located between the furnace and the pump. Analysis of the accumulated gaseous species by GC/MS revealed the presence of acetone, dmampH, and *N*,*N*,*N*′,*N*′-tetramethylethylene-1,2-diamine (Scheme 2). The gaseous species are the as same those of the $Cu(dmamp)_2$. Hence, the proposed mechanism of forming metallic nickel films from **1** is thought to be identical to that of $Cu(dmamp)_2$.[42] The proposed reaction pathway is shown in Scheme 3. The first step is the γ-hydrogen elimination of dmamp ligand to form the intermediates **A** and **B**. Intermediate **A** can then take one of two possible pathways. The first is the cyclization of the oxygen atom to produce the epoxide intermediate **C**. The other is a C–C cleavage resulting in intermediate **D** and acetone. The next step is the ring opening of **C** by the attack of **D**, and then *N*,*N*,*N*′,*N*′-tetramethylethylene-1,2-diamine and acetone are induced by C–C cleavage. On the other hand, in **B**, dmampH and pure Ni metal are produced by reductive elimination.

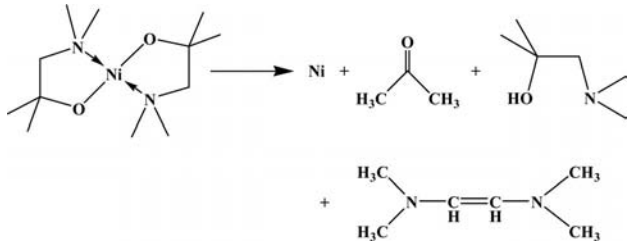

Scheme 2. Thermal decomposition products of complex **1**.

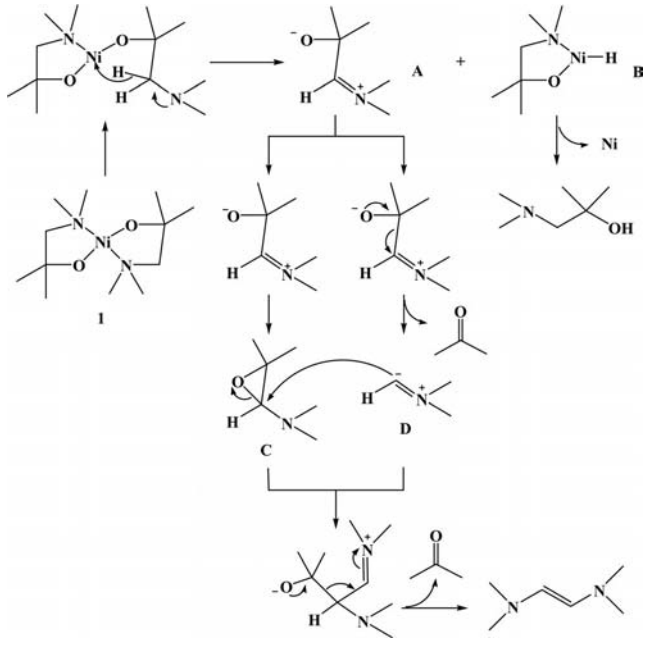

Scheme 3. Proposed thermal decomposition mechanism of complex **1**.

The Ni thin films deposited on SiO_2/Si(100) substrates by MOCVD using precursor **1** at 250 °C and 400 °C were examined by XRD and SEM. The XRD patterns show three peaks assigned to (010), (002), and (011) planes of hexagonal phase (JCPDS 45–1027) for the Ni thin films grown at 250 °C. In the films grown at 400 °C, two peaks corresponding to (111) and (200) planes of cubic phase (JCPDS 04-0850) were observed (Figure 6).

The SEM images of the Ni thin films grown at 250 and 400 °C are shown in Figure 7. The image for the 250 °C sample exhibits multiform shapes and various sized crystalline grains, whereas the 400 °C sample shows crystalline grains of various forms and a size distribution larger than that seen for the films grown at 250 °C.

XPS of a Ni film deposited from **1** on Si(111) at 250 °C showed the Ni $2p_{1/2}$, $2p_{3/2}$, 3s, 3p peaks, O 1s peak, and C 1s peak (Figure S1). XPS of a film deposited at 400 °C

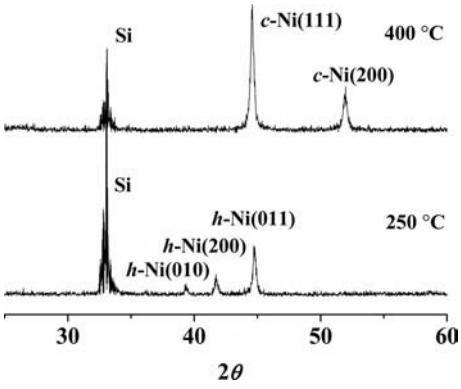

Figure 6. XRD patterns of Ni thin films grown from complex **1** at 250 °C and 400 °C.

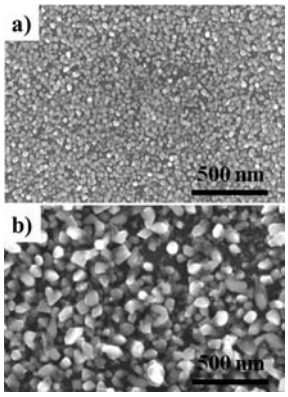

Figure 7. SEM images of Ni thin films grown from complex **1** at a) 250 °C and b) 400 °C.

showed the same peaks (Figure S2), however, the O 1s and C 1s peaks were of lesser intensity than those of film deposited at 250 °C. The film contained noticeable oxygen impurity, which is thought to be a contamination due to exposure of the sample to ambient conditions after the deposition process.

Conclusion

We have synthesized new Ni^{II} aminoalkoxide complexes, $Ni(dmamp)_2$ (**1**), $Ni(deamp)_2$ (**2**), and $Ni(emamp)_2$ (**3**). By thermal analysis, the Ni complexes showed high volatility. Melting points of the precursors decreased as the bulky alkyl groups on the nitrogen atom were substituted. The molecular structures of **1**–**3** reveal a square planar environment of Ni with the binding of two oxygen atoms and two nitrogen atoms in *trans* geometries. By TGA, the thermal properties of **1** are better than those of **2** and **3** and similar to known Ni precursors. Ni thin films were grown by the self-reduction of **1**. Through a GC/MS study of the generated gases during decomposition of **1**, the reaction shows the production of acetone, dmampH, and *N*,*N*,*N*′,*N*′-tetramethyl-ethene-1,2-diamine with nickel metal. Through the analysis the reaction pathway was proposed, metallic Ni is formed by γ-elimination and then reductive elimination. By MOCVD, hexagonal-phase Ni thin films were obtained at 250 °C, and cubic-phase Ni thin films were formed at 400 °C.

Experimental Section

General: All manipulations were performed under a dry, oxygen-free nitrogen or argon atmosphere using standard Schlenk techniques or in a glove box. All solvents were distilled under nitrogen from sodium/benzophenone prior to use. [D_6]Benzene and nickel(II) chloride hexahydrate were purchased from Aldrich and used without further purification. Nickel hexamine dichloride was prepared as reported in literature.[60] Functionalized bidentate alcohols, such as 1-(dimethylamino)-2-methyl-2-propanol [dmampH, $(CH_3)_2NCH_2C(CH_3)_2OH$], 1-(diethylamino)-2-methyl-2-propanol [deampH, $(CH_3CH_2)_2NCH_2C(CH_3)_2OH$], and 1-(ethylmethylamino)-2-methyl-2-propanol [emampH, $(CH_3CH_2)(CH_3)NCH_2\ C(CH_3)_2OH$] were synthesized by modified methods of references[54,61] and dried under nitrogen prior to use. ^1H and ^{13}C NMR spectra were recorded at 300 MHz on a Bruker DPX 300 MHz FT NMR spectrometer. All samples for NMR spectroscopy were contained in sealed NMR tubes and referenced using [D_6]benzene as internal standard. Infrared (IR) spectra were obtained with a Nicolet NEXUS FT-IR Spectrometer in a 4 mm KBr window or pellet with KBr. The samples were prepared in a glove box. Elemental analyses were performed by Thermoquest EA-1110 CHNS analyzer. Mass spectra were obtained on an Autospec mass spectrometer for electron impact (EI) mass spectra.

Synthesis of Nickel Aminoalkoxides $Ni(OCMe_2CH_2NRR')_2$ [R = R′ = Me (1); R = R′ = Et (2); R = Me, R′ = Et (3)]: The sodium salt of the amino alcohols (2 equiv.) [Na(dmamp) 2.37 g, 17.0 mmol (**1**); Na(deamp) 2.84 g, 17.0 mmol (**2**); Na(emamp) 2.60 g, 17.0 mmol (**3**)] was slowly added to a suspension of $[Ni(NH_3)_6]Cl_2$ (1.50 g, 8.5 mmol) in toluene (30 mL) and stirred under reflux for 8 h. After cooling, the reaction mixtures were filtered off and crude products were obtained by removal of all volatilities under vacuum. Analytically pure products were obtained by sublimation.

$Ni(dmamp)_2$ (1): Yield 2.17 g (88%), m.p. 118–120 °C. Sublimed at 70 °C (10^{-2} Torr). ^1H NMR (300 MHz, C_6D_6): δ = 1.38 [s, 12 H, -OC(CH_3)$_2$-], 1.73 [s, 4 H, -CH_2N(CH_3)$_2$], 2.32 [s, 12 H, -CH_2N-(CH_3)$_2$] ppm. ^{13}C NMR (75.7 MHz, C_6D_6): δ = 32.6 [-OC(CH_3)$_2$-], 51.5 [-CH_2N(CH_3)$_2$], 73.6 [-OC(CH_3)$_2$-], 78.3 [-CH_2N(CH_3)$_2$] ppm. FT-IR (KBr): $\tilde{\nu}$ = 2963 (s), 2911 (m), 2859 (m), 1467 (m), 1455 (m), 1438 (m), 1393 (w), 1367 (m), 1347 (m), 1295 (m), 1243 (w), 1195 (m), 1159 (m), 1112 (m), 1018 (m), 996 (m), 978 (m), 942 (s), 900 (w), 843 (m), 789 (w), 674 (s), 552 (w), 527 (w), 484 (w), 454 (w). MS: *m*/*z* (I%): 290 (39) [$Ni(dmamp)_2$], 275 (7) [$Ni(dmamp)_2$-CH_3], 174 (100) [Ni(dmamp)], 159 (21) [Ni(dmamp)-CH_3], 116 (30) [Ni(dmamp)-$CH_2N(CH_3)_2$], 58 (77) [dmamp-$CH_2N(CH_3)_2$]. $C_{12}H_{28}N_2NiO_2$ (291.08): calcd. C 49.52, H 9.70, N 9.62; found C 49.08, H 9.45, N 9.47.

$Ni(deamp)_2$ (2): Yield 2.32 g (79%), m.p. 52–53 °C. Sublimed at 70 °C (10^{-2} Torr). ^1H NMR (300 MHz, C_6D_6): δ = 1.34 [s, 12 H, -OC(CH_3)$_2$-], 1.68 [s, 12 H, -N(CH_2CH_3)$_2$], 1.87 [s, 4 H, -CH_2N-(CH_2CH_3)$_2$], 2.43 [br., s, 4 H, -N(CH_2CH_3)$_2$], 3.01 [br., s, 4 H, -N(CH_2CH_3)$_2$] ppm. ^{13}C NMR (75.7 MHz, C_6D_6): δ = 11.5 [-N(CH_2CH_3)$_2$], 34.0 [-OC(CH_3)$_2$-], 52.7 [-CH_2N(CH_2CH_3)$_2$], 67.1 [-N(CH_2CH_3)$_2$], 73.3 [-OC(CH_3)$_2$-] ppm. FT-IR (KBr): $\tilde{\nu}$ = 2971 (s), 2916 (m), 1459 (m), 1390 (m), 1371 (m), 1346 (m), 1282 (w), 1212 (m), 1171 (s), 1141 (m), 1080 (m), 1053 (m), 1032 (m), 971 (w), 901 (w), 786 (m), 674 (m), 592 (w), 532 (w), 444 (w), 419 (w).

MS: *m*/*z* (I%): 346 (15) [Ni(deamp)$_2$], 230 (25) [Ni(deamp)$_2$-$CH_2N(CH_2CH_3)_2$-$2CH_3$], 202 (39) [Ni(deamp)], 130 (44) [deamp-CH_3], 86 (100) [deamp-$2CH_2CH_3$], 58 (45) [deamp-$CH_2N(CH_2CH_3)_2$]. $C_{16}H_{36}N_2NiO_2$ (347.18): calcd. C 55.35, H 10.45, N 8.07; found C 50.95, H 9.69, N 8.60.

Ni(emamp)$_2$ (3): Yield 2.22 g (82%), m.p. 75–76 °C. Sublimed at 45 °C (10^{-2} Torr). ^{1}H NMR (300 MHz, C_6D_6): δ = 1.18, 1.62 [br. s, 12 H, -OC(CH_3)$_2$-], 1.72 (br. s, 6 H, -NCH$_2$CH_3), 1.44, 2.07 [br. d, 4 H, -CH_2N(Me)(Et)], 1.94, 2.89 (br. s, 4 H, -NCH_2CH$_3$), 2.54 (br. s, 6 H, -NCH_3) ppm. ^{13}C NMR (75.7 MHz, C_6D_6): δ = 11.9, 12.0 (-NCH$_2$CH_3), 32.3, 32.6, 34.3, 34.6 [-OC(CH_3)$_2$-], 48.8, 49.3 (-CH_2NCH$_3$), 56.2, 56.4 (-NCH_2CH$_3$), 72.8, 73.0 [-OC(CH$_3$)$_2$-], 73.6, 73.7 (-NCH$_3$) ppm. FT-IR (KBr): $\tilde{\nu}$ = 2963 (s), 2911 (m), 2859 (m), 1467 (m), 1455 (m), 1438 (m), 1393 (w), 1367 (m), 1347 (m), 1295 (m), 1243 (w), 1195 (m), 1159 (m), 1112 (m), 1018 (m), 996 (m), 978 (m), 942 (s), 900 (w), 843 (m), 789 (w), 674 (s), 552 (w), 527 (w), 484 (w), 454 (w). MS: *m*/*z* (I%): 318 (62) [Ni(emamp)$_2$], 303 (7) [Ni(emamp)$_2$-CH_3], 202 (75) [Ni(emamp)$_2$-$CH_2N(Me)(Et)$-CH_2CH_3–CH_3] 188 (93) [Ni(emamp)], 173 (23) [Ni(emamp)-CH_3], 72 (100) [emamp-N(CH_2CH_3)(CH_3)]. $C_{14}H_{32}N_2NiO_2$ (319.13): calcd. C 52.69, H 10.11, N 8.78; found C 48.94, H 9.69, N 7.98.

Crystal Structure Determination: Single crystals of the complexes were obtained from a saturated toluene solution of **1** at –30 °C, a saturated *n*-hexane solution of **2** at –30 °C or an *n*-hexane solution of **3** in a glass tube under reduced pressure. All of the crystals were subsequently mounted in thin-walled glass capillaries under Ar atmosphere that were sealed as a precaution against moisture/air sensitivity. Data collection for the crystals were performed on a Siemens SMART CCD equipped with a graphite crystal and incident-beam monochromator. The solutions of all structures were carried out by a combination of direct methods and Fourier techniques using SHELXTL program package[62] and refined by full-matrix least square methods based on unique reflection using SHELXL-97[62,63] with anisotropic temperature factors for all non-hydrogen atoms. Details of crystallographic data for **1**–**3** are summarized in Table 1.

Table 1. Crystal data and structure refinement for complexes **1**–**3**.

	1	**2**	**3**
Formula	$C_{12}H_{28}N_2NiO_2$	$C_{16}H_{36}N_2NiO_2$	$C_{14}H_{32}N_2NiO_2$
Crystal system	monoclinic	monoclinic	monoclinic
Space group	$P2_1/n$	$P2_1/c$	$P2_1/n$
a [Å]	5.8570(10)	18.950(6)	5.811(5)
b [Å]	18.108(2)	15.519(5)	17.457(5)
c [Å]	7.6710(10)	13.997(5)	8.516(5)
α [°]	90	90	90.000(5)
β [°]	111.07(2)	110.522(7)	108.393(5)
γ [°]	90	90	90.000(5)
V [Å^3]	759.18(18)	3855(2)	819.8(9)
Z	2	8	4
d_{calcd} [g cm^{-3}]	1.273	1.196	1.293
μ [mm^{-1}]	1.272	1.013	1.185
Reflections collected	1427	23899	5115
Unique reflections	1327	9111	1926
R_1 [$I > 2\sigma(I)$][a]	0.0525	0.0390	0.0210
wR_2 (all data)[b]	0.1402	0.1132	0.0577
GOF	1.027	1.040	1.062

[a] $R_1 = (\Sigma||F_o| - |F_c||)/\Sigma|F_o|$. [b] $wR_2 = [\Sigma\, w(F_o^2 - F_c^2)^2/\Sigma\, w(F_o^2)^2]^{1/2}$.

CCDC-796451 (for **1**), -796450 (for **2**), and -796452 (for **3**) contain the supplementary crystallographic data for this paper. These data can be obtained free of charge from The Cambridge Crystallographic Data Centre at www.ccdc.cam.ac.uk/data_request/cif.

Thermal Analysis: Thermogravimetric analyses and differential thermal analyses (TGA/DTA) for the newly synthesized complexes were investigated by Perkin–Elmer TGA7 apparatus. The TGA data of the complexes were obtained up to 800 °C at a heating rate of 10 °C/min under atmospheric pressure with N_2 as carrier gas.

Film Deposition: Ni thin films were grown on SiO_2/Si(100) substrates by MOCVD using Ni(dmamp)$_2$. Si(100) substrates were treated with piranha solution (H_2SO_4/H_2O_2 = 4:1) for 20 min and then rinsed several times with deionized water before loading. The base pressure of the deposition chamber was 2×10^{-5} Torr and the working pressure was increased to 3.5×10^{-2} Torr during the film deposition with Ar as carrier gas. The temperature of the precursor vessel was maintained at 70 °C. The substrate temperature was controlled at 250 and 400 °C. The surface morphology of the films was characterized by AFM (Nanoscope IV, Digital Instrument). X-ray diffraction (XRD) with the Cu-K_α radiation (λ = 1.541838 Å) was employed to investigate the crystallinity of the films.

Supporting Information (see footnote on the first page of this article): XP survey spectra of Ni film deposited on Si(111) at 250 and 400 °C with **1**.

Acknowledgments

This research was supported by the Converging Research Center Program through the Ministry of Education, Science and Technology (2010K000976)

[1] P. A. Premkumar, A. Dasgupta, P. Kuppusami, P. Parameswaran, C. Mallika, K. S. Nagaraja, V. S. Raghnathan, *Chem. Vap. Deposition* **2006**, *12*, 39–45.
[2] G. Dormans, *J. Cryst. Growth* **1991**, *108*, 806–816.
[3] J. Foggiato, W. S. Yoo, M. Ouaknine, T. Murakami, T. Fukada, *Mater. Sci. Eng. B* **2004**, *114–115*, 56–60.
[4] H. Sato, T. Minami, S. Takata, T. Yamada, *Thin Solid Films* **1993**, *236*, 27–31.
[5] S. A. Makhlouf, K. M. S. Khalil, *Solid State Ionics* **2003**, *164*, 97–106.
[6] S. Yamada, T. Yoshioka, M. Miyashita, K. Urabe, M. Kitao, *J. Appl. Phys.* **1988**, *63*, 2116–2119.
[7] S. Seo, M. J. Lee, D. H. Seo, E. J. Jeoung, D.-S. Suh, Y. S. Joung, I. K. Yoo, I. R. Hwang, S. H. Kim, I. S. Byun, J.-S. Kim, J. S. Choi, B. H. Park, *Appl. Phys. Lett.* **2004**, *85*, 5655–5657.
[8] J.-W. Park, J.-W. Park, D.-Y. Kim, J.-K. Lee, *J. Vac. Sci. Technol. A* **2005**, *23*, 1309–1313.
[9] P. O'Brien, J. Waters, *Chem. Vap. Deposition* **2006**, *12*, 620–626.
[10] A. Panneerselvam, G. Periyasamy, K. Ramasamy, M. Afzaal, M. A. Malik, P. O'Brien, N. A. Burton, J. Waters, B. E. van Dongel, *Dalton Trans.* **2010**, *39*, 6080–6091.
[11] Z. Y. Zhang, T. M. Nenoff, J. Y. Huang, D. T. Berry, P. P. Provencio, *J. Phys. Chem. C* **2009**, *113*, 1155–1159.
[12] R. Ferrando, J. Jelinek, R. L. Johnston, *Chem. Rev.* **2008**, *108*, 845–910.
[13] Y. W. Zhang, W. Y. Huang, S. E. Habas, J. N. Kuhn, M. E. Grass, Y. Yamada, P. Yang, G. A. Somorjai, *J. Phys. Chem. C* **2008**, *112*, 12092–12095.
[14] M. Watson, J. Banard, S. Hossain, M. Parker, *J. Appl. Phys.* **1993**, *73*, 5506–5508.
[15] M. Kitada, K. Yamamoto, N. Shimizu, *J. Magn. Magn. Mater.* **1993**, *124*, 243–245.
[16] T. Al-Kassab, M. Macht, V. Naundorf, H. Wollenberger, S. Chambreland, F. Danoix, D. Blavette, *Appl. Surf. Sci.* **1996**, *94/95*, 306–312.
[17] J. Willems, *Phillips J. Res. Suppl. 1* **1987**, 39, 1.
[18] N. Kuriyama, T. Sakai, H. Miyamura, H. Tanaka, H. Ishikawa, I. Uehara, *Vacuum* **1996**, *47*, 889–892.

[19] G. Adachi, H. Sakaguchi, K. Niki, N. Nagai, J. Shimokawa, *J. Less-Common Met.* **1985**, *108*, 107–114.
[20] T. Sakai, H. Ishikawa, H. Myamura, N. Kuriyama, *J. Electrochem. Soc.* **1991**, *138*, L4–L6.
[21] F. Goldberg, E. Knystautas, *Mater. Sci. Eng. B* **1996**, *40*, 185–189.
[22] E. Pellicer, A. Varea, S. Pané, B. J. Nelson, E. Menéndez, M. Estrader, S. Suriñach, M. D. Baró, J. Nogués, J. Sort, *Adv. Funct. Mater.* **2010**, *20*, 983–991.
[23] L. Mond, *J. Chem. Soc.* **1885**, 945.
[24] H. Carlton, J. Oxle, *AIChE J.* **1967**, *13*, 86–91.
[25] F. Fau-Canillac, F. Maury, *Surf. Coat. Technol.* **1994**, *64*, 21–27.
[26] G. T. Stauf, D. C. Driscoll, P. A. Dowben, S. Barfuss, M. Grade, *Thin Solid Films* **1987**, *153*, 421–430.
[27] G. J. M. Dormans, *J. Cryst. Growth* **1991**, *108*, 806–816.
[28] B. Fraser, A. Hampp, H. D. Kaesz, *Chem. Mater.* **1996**, *8*, 1858–1864.
[29] L. Brissonneau, C. Vahlas, *Chem. Vap. Deposition* **1999**, *5*, 135–142.
[30] T. Maruyama, T. Tago, *J. Mater. Sci.* **1993**, *28*, 5345–5348.
[31] R. van Hemert, L. Spenlove, R. Sievers, *J. Electrochem. Soc.* **1965**, *112*, 1123–1126.
[32] V. V. Bakovets, V. N. Mitkin, N. V. Gelfond, *Chem. Vap. Deposition* **2005**, *11*, 112–117.
[33] N. Bahlawane, P. A. Premkumar, K. Onwuka, G. Reiss, K. Kohse-Hoinghaus, *Microelectron. Eng.* **2007**, *84*, 2481–2485.
[34] B. S. Lim, A. Rahtu, J.-S. Park, R. G. Gordon, *Inorg. Chem.* **2003**, *42*, 7951–7958.
[35] B. S. Lim, A. Rahtu, R. G. Gordon, *Nat. Mater.* **2003**, *2*, 749–754.
[36] Z. Li, R. G. Gordon, V. Pallem, H. Li, D. V. Shenai, *Chem. Mater.* **2010**, *22*, 3060–3066.
[37] H. Kim, H.-B.-R. Lee, W.-J. Maeng, *Thin Solid Films* **2009**, *517*, 2563–2580.
[38] S. M. George, *Chem. Rev.* **2010**, *110*, 111–131.
[39] A. C. Jones, *J. Mater. Chem.* **2002**, *12*, 2576–2590.
[40] A. C. Jones, H. C. Aspinall, P. R. Chalker, R. J. Potter, K. Kukli, A. Rahtu, M. Ritala, M. Leskelä, *J. Mater. Chem.* **2004**, *14*, 3101–3112.
[41] L. McElwee-White, *Dalton Trans.* **2006**, 5323–5333.
[42] J. W. Park, H. S. Jang, M. Kim, K. Sung, S. S. Lee, T.-M. Chung, S. Koo, C. G. Kim, Y. Kim, *Inorg. Chem. Commun.* **2004**, *7*, 463–466.
[43] T. S. Yang, W. Cho, M. Kim, K.-S. An, T.-M. Chung, C. G. Kim, Y. Kim, *J. Vac. Sci. Technol. A* **2005**, *23*, 1238–1243.
[44] T. S. Yang, K.-S. An, E.-J. Lee, W. Cho, H. S. Jang, S. K. Park, Y. K. Lee, T.-M. Chung, C. G. Kim, S. Kim, J.-H. Hwang, C. Lee, N.-S. Lee, Y. Kim, *Chem. Mater.* **2005**, *17*, 6713–6718.
[45] Y.-H. You, B.-S. So, J.-H. Hwang, W. Cho, S. S. Lee, T.-M. Chung, C. G. Kim, K.-S. An, *Appl. Phys. Lett.* **2006**, *89*, 222105.
[46] W. Cho, K.-S. An, T.-M. Chung, C. G. Kim, B.-S. So, Y.-H. You, J.-H. Hwang, D. Jung, Y. Kim, *Chem. Vap. Deposition* **2006**, *12*, 665–669.
[47] K.-C. Min, M. Kim, Y.-H. You, S. S. Lee, Y. K. Lee, T.-M. Chung, C. G. Kim, J.-H. Hwang, K.-S. An, N.-S. Lee, Y. Kim, *Surf. Coat. Technol.* **2007**, *201*, 9252–9255.
[48] S. S. Lee, H.-M. Lee, M.-J. Park, K.-S. An, J. Kim, J.-H. Lee, T.-M. Chung, C. G. Kim, *Bull. Korean Chem. Soc.* **2008**, *29*, 1491–1494.
[49] P. Werndrup, S. Gohil, V. G. Kessler, M. Kritikos, L. G. Hubert-Pfalzgraf, *Polyhedron* **2001**, *20*, 2163–2169.
[50] T. Kada, M. Ishikawa, H. Machida, A. Ogura, Y. Ohshita, K. Soai, *J. Cryst. Growth* **2005**, *275*, e1115–e1119.
[51] A. Pande, *Synlett* **2005**, *6*, 1042–1043.
[52] F. Emmenegger, C. W. Schlaepfer, H. Stoeckli-Evans, M. Piccand, H. Piekarski, *Inorg. Chem.* **2001**, *40*, 3884–3888.
[53] M. L. Morris, R. W. Moshier, R. E. Sievers, *Inorg. Chem.* **1963**, *2*, 411–412.
[54] A. Heydari, M. Mehrdad, A. Maleki, N. Ahmadi, *Synthesis* **2004**, 1563–1565.
[55] X. He, Y. Yao, X. Luo, J. Zhang, Y. Liu, L. Zhang, Q. Wu, *Organometallics* **2003**, *22*, 4952–4957.
[56] C. Tsiamis, A. G. Hatzidimitriou, M. Uddin, *Inorg. Chim. Acta* **1996**, *249*, 105–109.
[57] L. G. Hubert-Pfalzgraf, V. G. Kessler, J. Vaissermann, *Polyhedron* **1997**, *16*, 4197–4203.
[58] G. Malandrino, L. M. S. Perdicaro, G. Condorelli, I. L. Fragalà, P. Rossi, P. Dapporto, *Dalton Trans.* **2006**, 1101–1106.
[59] P. A. Premkumar, R. Pankajavalli, O. M. Sreedharan, V. S. Raghunathan, K. S. Nagaraja, C. Mallika, *Mater. Lett.* **2004**, *58*, 2256–2260.
[60] G. W. Watt, *Inorg. Synth.* **1950**, *3*, 194.
[61] R. Anwander, F. C. Munck, T. Priermeier, W. Scherer, O. Runte, W. A. Herrmann, *Inorg. Chem.* **1997**, *36*, 3545–3552.
[62] G. M. Sheldrick, *Acta Crystallogr., Sect. A* **2008**, *64*, 112–122.
[63] G. M. Sheldrick, *SHELX97, Program for Crystal Structure Refinement*, University of Göttingen, Göttingen, Germany, **1997**.

Received: October 23, 2010
Published Online: March 1, 2011

